Production of Reactive Oxygen Species by Complex I (NADH:Ubiquinone Oxidoreductase) from Escherichia coli and Comparison to the Enzyme from Mitochondria †

ARTICLE *in* BIOCHEMISTRY · APRIL 2008

Impact Factor: 3.02 · DOI: 10.1021/bi702243b · Source: PubMed

Production of Reactive Oxygen Species by Complex I (NADH:Ubiquinone Oxidoreductase) from *Escherichia coli* and Comparison to the Enzyme from Mitochondria[†]

Daria Esterházy,[‡] Martin S. King, Gregory Yakovlev, and Judy Hirst*

Medical Research Council Dunn Human Nutrition Unit, Wellcome Trust/MRC Building, Hills Road, Cambridge, CB2 0XY, United Kingdom

Received November 12, 2007; Revised Manuscript Received January 11, 2008

ABSTRACT: The generation of reactive oxygen species by mitochondrial complex I (NADH:ubiquinone oxidoreductase) is considered a significant cause of cellular oxidative stress, linked to neuromuscular diseases and aging. Defining its mechanism is important for the formulation of causative connections between complex I defects and pathological effects. Oxygen is probably reduced at two sites in complex I, one associated with NADH oxidation in the mitochondrial matrix and the other associated with ubiquinone reduction in the membrane. Here, we study complex I from *Escherichia coli*, exploiting similarities and differences in the bacterial and mitochondrial enzymes to extend our knowledge of O_2 reduction at the active site for NADH oxidation. *E. coli* and bovine complex I reduce O_2 at essentially the same rate, with the same potential dependence (set by the NAD^+/NADH ratio), showing that the rate-determining step is conserved. The potential dependent rate of H_2O_2 production does not correlate to the potential of the distal [2Fe−2S] cluster N1a in *E. coli* complex I, excluding it as the point of O_2 reduction. Therefore, our results confirm previous proposals that O_2 reacts with the fully reduced flavin mononucleotide. Assays for superoxide production by *E. coli* complex I were prone to artifacts, but dihydroethidium reduction showed that, upon reducing O_2, it produces approximately 20% superoxide and 80% H_2O_2. In contrast, bovine complex I produces 95% superoxide. The results are consistent with (but do not prove) a specific role for cluster N1a in determining the outcome of O_2 reduction; possible reaction mechanisms are discussed.

Complex I (NADH:ubiquinone oxidoreductase) is the first enzyme of the membrane-bound electron-transport chain in many aerobically respiring organisms (*1–3*). It oxidizes NADH, reduces ubiquinone, and conserves the potential difference as a proton motive force (PMF)[1] across the inner mitochondrial or cytoplasmic membrane. The substrates and cofactors of complex I have the lowest potentials in the respiratory chain; therefore, it is not surprising that complex I is increasingly recognized as a major contributor to reactive oxygen species (ROS) formation in mitochondria (*4–6*). ROS, such as the superoxide anion and hydrogen peroxide, are a topic of intense current interest, because they are a major cause of cellular oxidative stress and thought to contribute to many pathological conditions including Parkinson's and other neurodegenerative diseases, ischemia reperfusion injury, atherosclerosis, and the aging process (*4, 6–9*). Complex I deficiencies have been identified in a wide range of such pathologies and linked to both increased oxidative stress and deficient energy production (see, for example, refs *10–13*). Consequently, it is important to define the mechanism of ROS production by complex I, to understand the relationships between enzyme activity and pathology, and to propose rational strategies for how defects may be addressed. There is considerable experimental support for two distinct (but not mutually exclusive) mechanisms of ROS production by mitochondrial complex I. First, studies on the isolated enzyme proposed that superoxide is formed by the reduced flavin mononucleotide (FMN) in the active site for NADH oxidation, although the participation of the distal [2Fe−2S] cluster in the 24 kDa subunit (N1a) could not be discounted unambiguously (*14, 15*). In mitochondria, this mechanism is supported by correlations between the $NAD(P)^+$ potentials and ROS generation (see below) (*16–19*). Second, superoxide production by ubisemiquinone intermediates, which persist only in the presence of a PMF (*20*), correlates to observations of ubisemiquinone radicals by electron paramagnetic resonance (EPR) (*21*). Here, we describe studies of ROS production by complex I isolated from *Escherichia coli* and compare the results to those reported previously for complex I from bovine heart mitochondria (*14*). Because we study only the isolated complexes, our experimental system is simple and precise, but we are unable to impose a PMF and therefore do not observe O_2 reduction by any ubisemiquinone intermediates.

[†] This research was funded by The Medical Research Council.

* To whom correspondence should be addressed: Medical Research Council Dunn Human Nutrition Unit, Wellcome Trust/MRC Building, Hills Road, Cambridge, CB2 0XY, U.K. Telephone: +44-1223-252810. Fax: +44-1223-252815. E-mail: jh@mrc-dunn.cam.ac.uk.

[‡] Current address: Institute of Molecular Systems Biology, ETH Zurich, CH-8093 Zurich, Switzerland.

[1] Abbreviations: ac cyt *c*, partially acetylated cytochrome *c*; CAT, catalase; CI, complex I; DHE, dihydroethidium; DHR, dihydrorhodamine; EPR, electron paramagnetic resonance; FeS, iron−sulfur cluster; FMN, flavin mononucleotide; HRP, horseradish peroxidase; PMF, proton motive force; SOD, superoxide dismutase.

10.1021/bi702243b CCC: $40.75
Published on Web 02/29/2008

Table 1: Reduction Potentials for [2Fe−2S] Cluster N1a and the Flavin in the Complexes I from *E. coli* and Bovine Mitochondria and Comparison to Values from the Potential Dependence of the Rate of H_2O_2 Production[a]

	reduction potentials from the literature			reduction potentials determined from variations in H_2O_2 production		
	E_{N1a} (V)	FMN E_{AV} (V)	FMN ΔE (V)	E_m (Figure *3*A) (V)	FMN E_{AV} (Figure *3*B) (V)	FMN ΔE (Figure *3*B) (V)
E. coli complex I	−0.25[b] (*22*)	nd	nd	−0.330	−0.314	−0.025
bovine complex I	<−0.4[c] (−0.37) (*23*) (−0.46) (*24*)	−0.365 (*25*)	0.09 (*25*)	−0.360 (*14*)	−0.357 (*14*)	0.080 (*14*)

[a] $E_{AV} = (E_{F1} + E_{F2})/2$, and $\Delta E = E_{F2} - E_{F1}$ (see Figure 3B). [b] Value from intact *E. coli* complex I; a pH-independent value reported at pH 7. [c] The reduction potential of [2Fe−2S] cluster N1a in bovine complex I is unclear. The EPR signal N1a is not observed in NADH-reduced bovine complex I (*14*), suggesting that N1a has a potential below −0.4 V; the generally accepted value reported in the literature, −0.37 V (*23*), was derived from an EPR signal with *g* values that do not match those of N1a. The [2Fe−2S] cluster in the over-expressed bovine 24 kDa subunit has a reduction potential that is dependent on pH and ionic strength (−0.46 V at pH 7.5, 0.1 M NaCl) (*24*). However, this value may be modulated by the different protein environment; the analogous value from the over-expressed *E. coli* NuoE subunit, −0.32 V, is lower than that exhibited by the cluster in the intact enzyme.

The mechanism of O_2 reduction by mitochondrial complex I determined previously (see ref *14*) can be simplified by considering it in two parts: *rate* and *fate*.

The *rate* of O_2 reduction is determined by a slow, second-order reaction between a reduced cofactor in the enzyme (probably the fully reduced flavin) and O_2, to produce superoxide. It depends linearly upon the O_2 and enzyme concentrations and on the fraction of the enzyme in which the cofactor is reduced and available. The oxidation states of the cofactors in complex I can be "poised" using NADH and NAD^+; because the reactions of complex I with NADH and NAD^+ are much faster than its reaction with O_2, they are considered to be at equilibrium. Thus, the dependence of the rate of superoxide production on potential is equivalent to a redox titration of the O_2-reducing cofactor. In bovine complex I, the potential of the cofactor was found to be close to reported potentials for the flavin and [2Fe−2S] cluster N1a (see Table 1). Although further evidence supported the fully reduced flavin in an unoccupied active site as the reductant of O_2, [2Fe−2S] cluster N1a could not be discounted unambiguously. Here, we compare the rate and potential dependence of O_2 reduction by the bovine and *E. coli* complexes I. We aim to determine whether the mechanism of O_2 reduction is conserved and to exploit the fact that [2Fe−2S] cluster N1a has a higher potential in *E. coli* complex I than in bovine complex I (see Table 1) to rule it out unambiguously as the reductant of O_2.

If O_2 reacts with the fully reduced flavin, then the *fate* of the nascent superoxide is decided by its rate of dissociation from the active site, relative to its rate of reduction by the second electron from the flavin semiquinone, to produce H_2O_2 (*26*–*28*). In bovine complex I, more than 90% of the nascent superoxide escapes as superoxide (*14*). The recent structure of the hydrophilic domain of complex I showed that [2Fe−2S] cluster N1a is on the opposite (distal) side of the flavin from the ubiquinone-binding site and has no obvious role in energy transduction (*29*). It has been suggested to minimize the lifetime of the flavin semiquinone and thus O_2 reduction by temporarily accepting the "second" electron during turnover (*3*). Here, we ask whether *E. coli* complex I produces predominantly superoxide or H_2O_2. Consequently, we aim to exploit the different reduction potentials of [2Fe−2S] cluster N1a in the *E. coli* and bovine enzymes to question its possible role in determining the outcome of O_2 reduction.

EXPERIMENTAL PROCEDURES

Preparation of E. coli and Bovine Complex I and the NuoE Subunit. Complex I was purified from *E. coli* strain BL21 as described previously (*30*), except that a DEAE-Sepharose fast-flow column was used for the second ion-exchange chromatography step and a Superose 6 10/300 GL column (GE Healthcare Biosciences) was used for gel filtration. Complex I from bovine mitochondria was purified as described previously (*31*). Enzyme concentrations were determined using the Pierce bicinchoninic acid assay or from the FMN concentrations, determined fluorometrically (*32*). The NuoE subunit from *E. coli* complex I (homologous to the bovine 24 kDa subunit) was overexpressed and prepared as described previously (*24*).

Measurement of the Rate of H_2O_2 Production Using Amplex Red. Rates of H_2O_2 production were determined as described previously (*14*) using a diode array UV–vis spectrometer (Ocean Optics) or a plate reader (Molecular Devices). Typical assays comprised 20 mM Tris-HCl (pH 7.5), 30 μM NADH (Sigma), 0.4 unit mL^{-1} horseradish peroxidase (HRP, Amresco), 10 μM Amplex Red (Invitrogen), and 0−0.03 mg mL^{-1} complex I at 30 °C. The oxidation of Amplex Red to resorufin was monitored at 557–620 nm ($\epsilon = 51.6\ mM^{-1}\ cm^{-1}$), and NADH oxidation was quantified in separate assays for comparison ($\epsilon_{340-420} = 6.22\ mM^{-1}\ cm^{-1}$). Superoxide dismutase (SOD, from bovine erythrocytes, Sigma) and catalase (CAT, from bovine liver, Sigma) were added to 10 units mL^{-1} and 1000 units mL^{-1}, respectively, when appropriate. Redox titrations were carried out in 30 μM NADH, by varying the NAD^+ concentration; NADH samples were repurified anaerobically immediately before use, as described previously (*14*).

Assays for the Detection of Superoxide. All assays were carried out in 20 mM Tris-HCl (pH 7.5) and 30 μM NADH; SOD was added to 10 units mL^{-1} when required. Assays using 50 μM partially acetylated equine heart cytochrome *c* (ac cyt *c*; $\epsilon_{550-541} = 18.0\ mM^{-1}\ cm^{-1}$, Sigma) were carried out as described previously (*14*). WST-1 (water-soluble tetrazolium salt-1, 4-[3-(4-iodophenyl)-2-(4-nitrophenyl)-*H*-5-tetrazolio]-1,3-benzene disulfonate sodium salt, Sigma) reduction to its formazan form was monitored spectroscopically ($\epsilon_{438} = 37.0\ mM^{-1}\ cm^{-1}$) at 30 °C, in 50 μM WST-1 and 0−0.05 mg mL^{-1} complex I (*33*). Luminol (5-amino-2,3-dihydro-1,4-phthalazine-dione) chemiluminescence was measured using a Berthold Autolumat Plus luminometer at room temperature, using 0−0.05 mg mL^{-1} complex I and luminol (Fluka) at 25−100 μM (*34*). Coelenterazine (8-benzyl-2-(4-hydroxybenzyl)-6-(4-hydroxyphenyl)imidazo [1,2-*a*]pyrazin-3(7*H*)-one, Calbiochem) chemiluminescence was monitored similarly using 2 μM coelenterazine and 0−0.02 mg mL^{-1} complex I (*35*). The conversion of dihydroethidium

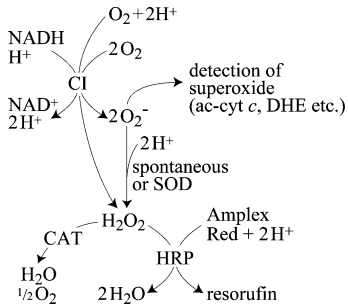

FIGURE 1: Generation of superoxide and/or hydrogen peroxide by complex I and their interconversion and detection. CI, complex I, is reduced by NADH and oxidized by O_2, to form either superoxide or H_2O_2. The superoxide can be detected (using, for example, ac cyt *c* or DHE) or dismutated to H_2O_2 (either spontaneously or by SOD). The H_2O_2 can be detected by Amplex Red or dismutated by CAT.

(Fluka) to ethidium, intercalated into DNA, was monitored by fluorescence at 30 °C, using a Shimadzu RF 5301PC spectrofluorometer and excitation and emission wavelengths of 396 and 590 nm, respectively (*36*). Typical concentrations were 50 μM dihydroethidium, 50 μg mL^{-1} DNA (from salmon sperm, Sigma), and 0−0.03 mg mL^{-1} complex I. Superoxide-dependent peroxynitrite formation (*37*) was detected by the oxidation of dihydrorhodamine 123 (Sigma) to rhodamine, monitored fluorometrically as above, using excitation and emission wavelengths of 500 and 536 nm, respectively (*38*). DETA-NONOate (3,3-bis(aminoethyl)-1-hydroxy-2-oxo-1-triazene, Sigma) was added to 250 μM and incubated in the assay buffer for 10 min before the reaction was initiated, to generate NO. The assays used 50 μM dihydrorhodamine 123 and 0−0.05 mg mL^{-1} complex I.

EPR Spectroscopy. Complex I samples were dialyzed anaerobically against 20 mM Tris-HCl at pH 7.5 and 0.1 mM NADH for 1 h at 4 °C and then split into two aliquots. One aliquot was reduced further by the addition of 5 mM NADH and frozen immediately; the other aliquot was poised at −0.3 V by the addition of 0.24 mM NADH and 4.76 mM NAD^+ (taking into account the NADH in the dialysis) and also frozen immediately. The complex I concentration in both samples was the same. EPR spectra were recorded on a Bruker EMX X-band spectrometer using an ER 4119HS high-sensitivity cavity maintained at low temperature by an Oxford Instruments ESR900 continuous flow liquid helium cryostat; the sample temperature was measured with a calibrated Cernox resistor (Lake Shore Cryotronics, Inc.).

RESULTS AND DISCUSSION

Rate of H_2O_2 Production by E. coli Complex I and Comparison to the Bovine Enzyme. The HRP-dependent oxidation of Amplex Red to resorufin was used to quantify H_2O_2 production by purified *E. coli* complex I in the presence of NADH and O_2 (see Figure 1). The assays detected the H_2O_2 produced directly and by superoxide dismutation and were carried out in 30 μM NADH, under atmospheric O_2, at pH 7.5 and 30 °C. These conditions were optimized previously to assay H_2O_2 production by complex I from bovine mitochondria (*14*); separate experiments confirmed that *E. coli* complex I retained its NADH:ferricyanide oxidoreductase activity over the course of the experiment and that the apparent K_M for NADH (in the NADH:O_2 oxidoreductase reaction) was significantly lower than 30 μM (the reaction between NADH and complex I is not rate-limiting). Both the rates of resorufin formation and NADH oxidation linearly depended upon the enzyme concentration (between 0 and 0.03 mg mL^{-1}), and a ratio of 1 NADH to 1 ± 0.1 H_2O_2 was observed at all concentrations. The addition of catalase (CAT) essentially abolished H_2O_2 detection, confirming the specificity of the assay, and the addition of superoxide dismutase (SOD) had little effect (see Table 2). These results confirm that all of the electrons from NADH oxidation are conserved in H_2O_2 formation. The rate of H_2O_2 production was 24.2 ± 3.8 H_2O_2 min^{-1}, comparable to the equivalent value from bovine complex I (see Table 2).

Table 2: Rates of NADH Oxidation and H_2O_2 Production by Complex I from *E. coli* and Comparison to Data from the Bovine Enzyme[a]

measurement (min^{-1})		*E. coli* complex I	bovine complex I (*14*)
CI plus NADH	H_2O_2 formation	24.2 ± 3.6	21.1 ± 2.7
	NADH oxidation	25.1 ± 3.8	20.9 ± 0.8
CI plus NADH and SOD	H_2O_2 formation	23.6 ± 3.8	21.1 ± 2.9
CI plus NADH and CAT	H_2O_2 formation	1.1 ± 1.0	1.9 ± 0.8
NADH only	H_2O_2 formation	<0.01	0.003 ± 0.002

[a] CI, complex I. Conditions: 20 mM Tris-HCl at pH 7.5 and 30 °C, 30 μM NADH, 0.4 unit mL^{-1} HRP, and 10 μM Amplex Red. SOD was added to 10 units mL^{-1}, and CAT was added to 1000 units mL^{-1}, when required. Values reported in the absence of complex I are in equivalent units for comparison.

The similar rates of H_2O_2 production observed (under the same conditions) suggest that bovine complex I has not evolved additional mechanisms for minimizing O_2 reduction and that its many supernumerary subunits (*39*) do not hinder the access of O_2 to the active site. However, the physiological rates of H_2O_2 production by the two enzymes respond to the cellular conditions and thus may differ significantly. Interestingly, complex I is considered an important contributor to ROS production in mitochondria (*4–6*), although the low O_2 concentration (*40*) and the high potential of the NAD^+ pool both act to decrease its rate of O_2 reduction (*14*). In contrast, the intracellular O_2 concentration in *E. coli* may be much higher (*41*), but ROS production is dominated by NADH dehydrogenase II (NDH-II), because it has a higher rate of O_2 reduction (∼140 min^{-1} under atmospheric O_2) (*42*) and a relatively high flavin potential (enabling it to reduce O_2 over a greater range of conditions).

The Mechanism of O_2 Reduction Is Conserved in the E. coli and Bovine Complexes I. Figure 2 shows that the rate of H_2O_2 formation by *E. coli* complex I strongly depends upon the NAD^+/NADH ratio, plotted using E_{SET}, the Nernst potential for the NAD^+/NADH couple, defined using E_{NAD^+} = −0.335 V at pH 7.5 (eq 1)

$$E_{SET} = E_{NAD^+} - \frac{RT}{2F}\ln\left\{\frac{[NADH]}{[NAD^+]}\right\} \quad (1)$$

Similar results were observed previously for complex I from bovine mitochondria (*14*) (see Figure 2 also). Together with their similar rates of O_2 reduction, these results suggest strongly that O_2 reduction by both enzymes is defined by the same rate-determining step. The data from bovine complex I were interpreted using "pre-equilibrium" models

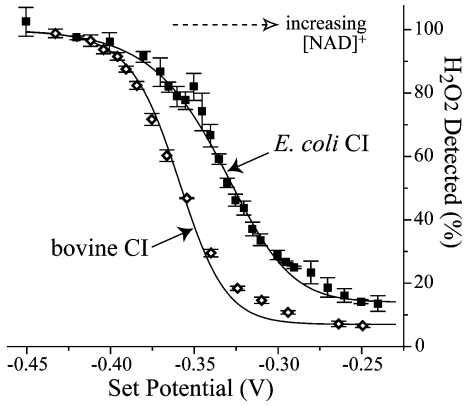

FIGURE 2: Comparison of H_2O_2 production by the complexes I from *E. coli* and bovine mitochondria, as a function of the Nernst potential set by the NAD^+/NADH ratio. H_2O_2 production was measured by the HRP/Amplex Red assay, in the presence of 30 μM NADH and varying concentrations of NAD^+ (up to 40 mM). The set potential (E_{SET}) was calculated from the NAD^+/NADH ratio using eq 1 and E_{NAD^+} = –0.335 V. Rates are expressed as a percentage of the rate in NADH only (see Table 2) and were modeled using eq 2 (see Table 1 for parameter values). Data for the bovine enzyme are from Kussmaul and Hirst (*14*). Data points for the *E. coli* enzyme are the average values from four independent experiments (error bars, ± standard deviation). Conditions: 20 mM Tris-HCl at pH 7.5 and 30 °C.

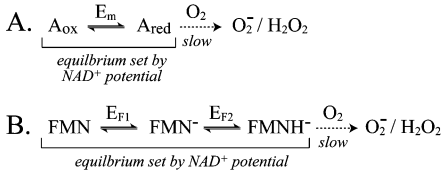

FIGURE 3: Rate of reduction of O_2 is determined by an equilibrium distribution of reactive and nonreactive states and a slow bimolecular reaction. (A) Simple equilibrium between the oxidized and reduced forms of species A [determined by the reduction potential of A (E_m) and the set potential, eq 1] determines the rate of O_2 reduction. Species in equilibrium are marked with the horizontal bracket. (B) Equilibrium comprises three oxidation states for the flavin cofactor (bracketed) and is determined by the two flavin potentials (eq 2) and the set potential (eq 1).

that rely on the reactions between complex I and NADH or NAD^+ being much faster than the reaction with O_2, so that O_2 reduction does not deplete the "active" species or perturb the equilibrium with NADH and NAD^+ significantly (see ref *14*). For *E. coli* complex I (as for bovine complex I), rates of NADH oxidation observed using artificial electron acceptors, such as ferricyanide and hexaammine ruthenium, are more than 3 orders of magnitude faster than O_2 reduction (*22, 30, 43*).

Flavin and Not Cluster N1a Is the Source of Electrons for O_2 Reduction. The simplest pre-equilibrium model to explain the data in Figure 2 (Figure 3A) proposes that the reduction state of the cofactor, which controls the donation of electrons to O_2, is set by the potential of the NADH/NAD^+ pool. In this model, the potential of the cofactor is at the midpoint of the titration curve (see Figure 2). In *E. coli* complex I, the apparent potential of the donating cofactor is slightly higher than in the bovine enzyme (−0.33 V in *E. coli* versus −0.36 V in the bovine enzyme). It is clear that its potential does not match the potential of [2Fe−2S] cluster N1a in *E. coli* complex I (see Table 1), and the EPR spectra shown in Figure 4 support this conclusion. They are from *E. coli* complex I poised at ∼ −0.4 V (NADH only) and

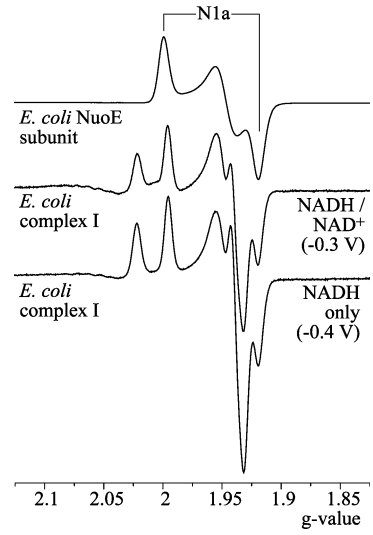

FIGURE 4: EPR spectra showing that the [2Fe−2S] cluster in the NuoE subunit of *E. coli* complex I is essentially reduced fully at –0.3 V. (Bottom) *E. coli* complex I (∼10 μM) reduced anaerobically in 5 mM NADH to ca. –0.4 V. (Middle) *E. coli* complex I (at the same concentration) reduced anaerobically in 0.24 mM NADH and 4.76 mM NAD^+ to –0.3 V. (Top) the overexpressed NuoE subunit, reduced with sodium dithionite, for comparison (*24*). The intensity of the N1a signal, from the [2Fe−2S] cluster in NuoE, is increased by only 14% in the –0.4 V sample, showing that the cluster is essentially fully reduced at –0.3 V. Signal N1b, from the [2Fe−2S] cluster in the NuoG subunit, is present in the complex I spectra also, and it is increased by 40% in the –0.4 V sample. Conditions: microwave power, 1 mW; conversion time, 81.92 ms; time constant, 20.48 ms; modulation amplitude, 10 G; microwave frequency, ∼9.38 MHz.

−0.3 V (using a ratio of NADH and NAD^+ set by the Nernst equation), corresponding to set potentials of high and low H_2O_2 production (see Figure 2). Signal N1a is clearly apparent in both cases, with comparable intensity, showing unambiguously that [2Fe−2S] cluster N1a is not the reductant of O_2 in *E. coli* complex I. Consequently, it can be dismissed as the reductant of O_2 in bovine complex I also. None of the EPR detectable FeS clusters in bovine complex I (EPR signals N1b, N3, N4, N5, and N2) have redox states that correlate to the titration curve for H_2O_2 production; therefore, they were ruled out previously as cofactors that react with O_2 (*14*). In addition, the bovine Fp subcomplex (containing only the flavin and the clusters with EPR signals N1a and N3) displays a very similar titration curve to the intact enzyme (E_m = −0.325 ± 0.02 V, data not shown). As discussed earlier, the titration curves in Figure 2 are sigmoidal and not peak-shaped, corresponding to the fully reduced flavin and not the semiquinone radical (*14*). We conclude that the fully reduced flavin cofactor in complex I is the cofactor that reduces O_2.

Interpreting the Dependence of H_2O_2 Production on Reduction Potential. The scheme in Figure 3B shows how the rate of O_2 reduction is proportional to the concentration of the fully reduced flavin, $FMNH^-$ (or $FMNH_2$), and eq 2 defines how the concentration of the fully reduced flavin depends upon the set potential, E_{SET} (see eq 1). Figure 2 shows that the data for both *E. coli* and bovine complex I (*14*) can be modeled accurately using Figure 3B and eq 2.

$$E_{SET} = E_{F1} - \frac{RT}{F}\ln\left\{\frac{[FMN^-]}{[FMN]}\right\} = E_{F2} - \frac{RT}{F}\ln\left\{\frac{[FMNH^-]}{[FMN^-]}\right\} \quad (2)$$

The data are characterized by E_{AV}, the average of the two one-electron FMN potentials ($E_{AV} = (E_{F1} + E_{F2})/2$), and ΔE, the separation between them ($\Delta E = E_{F2} - E_{F1}$) (see Table 1). E_{AV} and ΔE define the two-electron reduction potential of the flavin and the thermodynamic stability of the flavin semiquinone. The two-electron potential of the flavin in *E. coli* complex I from Figure 2 is −0.314 V, slightly higher than the equivalent value reported previously for bovine complex I (−0.357 V) (*14*). The value from bovine complex I matches independent data from EPR very well (see Table 1), but there is currently no complementary data available for the *E. coli* enzyme. It is possible that *E. coli* complex I binds the oxidized flavin less selectively than the bovine enzyme does (*25*). Figure 2 also shows that the data curve for *E. coli* complex I is broader ($\Delta E = -0.025$ V) than that for the bovine enzyme ($\Delta E = 0.08$ V), indicating that the flavin semiquinone is more thermodynamically stable in *E. coli* complex I. Finally, it is likely that O_2 only reacts with the reduced flavin in the absence of bound nucleotide. To define accurately how the level of fully reduced and available flavin is determined in each enzyme, it will be necessary to define dissociation constants for both NADH and NAD^+ for each oxidation state of the flavin, the equilibrium constant for hydride transfer, and the two one-electron flavin potentials (*14*). Little is known about the values of most of these thermodynamic constants, particularly for the *E. coli* enzyme.

Measuring the Ratio of Superoxide and H_2O_2 Produced by E. coli Complex I. The H_2O_2 produced by *E. coli* complex I and detected using Amplex Red comprises the H_2O_2 produced directly and the H_2O_2 produced by dismutation (see Figure 1). Six different methods of superoxide detection were tested, to differentiate the two pathways (*44–46*). Only one, dihydroethidium oxidation, provided satisfactory results.

The reduction of ac cyt *c* was used successfully to quantify superoxide production from bovine complex I (*14*), but the *E. coli* enzyme was found to catalyze NADH:ac cyt *c* oxidoreduction directly. In addition, ac cyt *c* decreased the rates of NADH:ferricyanide oxidoreduction and O_2 reduction (determined as the sum of Amplex Red oxidation and ac cyt *c* reduction). It is likely that ac cyt *c* blocks the *E. coli* complex I active site, precluding superoxide quantification. As an alternative oxidant for superoxide, a water-soluble tetrazolium salt, WST-1, was tested (*33*). However, it was reduced rapidly and directly, even by bovine complex I in the absence of O_2; similar observations have been described previously (*44*).

In preliminary experiments using bovine complex I, luminol (*34*) displayed apparent rates of superoxide detection that increased spontaneously during the assays and nonlinearly depended upon complex I concentration; its autocatalytic behavior has been described previously (*46*). For bovine complex I, superoxide detection by coelenterazine (*35*) linearly depended upon the enzyme concentration, was SOD-sensitive, and displayed negligible background rates. However, it could not be used to quantify superoxide production by *E. coli* complex I because the apparent rate of superoxide production exponentially depended upon the enzyme concentration, detection was only partially SOD-sensitive, and rates were at least an order of magnitude higher than for the bovine enzyme (despite their similar overall H_2O_2 production). Neither SOD, desferroxamine, or the absence of NADH, decreased the high background rates observed,

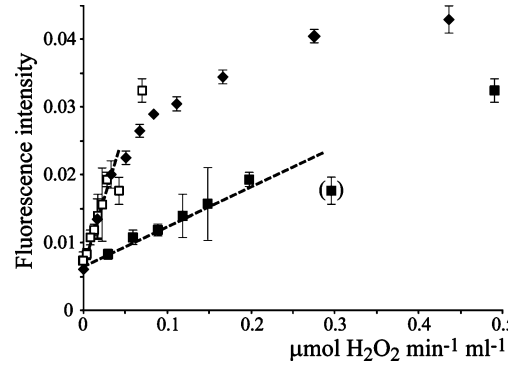

FIGURE 5: Determination of the relative rates of superoxide production by bovine and *E. coli* complexes I using DHE. Measurements of the relative fluorescence intensity of the ethidium product of dihydroethidium oxidation (intercalated into DNA) are shown as a function of H_2O_2 production, measured using the Amplex Red assay; enzyme concentrations varied between approximately 0 and 0.03 mg mL^{-1}. ◆, bovine complex I; ■, *E. coli* complex I; □, *E. coli* complex I data set mapped onto the bovine data set (abscissa divided by 7). Dashed lines: linear regression for the data with low superoxide production (the bracketed data point was excluded). Conditions: 20 mM Tris-HCl (pH 7.5), 30 μM NADH, 50 μM dihydroethidium, and 50 μg mL^{-1} DNA at 30 °C.

although they were not exhibited by "adjacent" protein fractions from the purification or by the enzyme buffer. The reason for this different behavior is not understood at present.

Dihydroethidium (DHE) is oxidized by superoxide, in two one-electron steps, to ethidium, which can be intercalated into DNA and detected by fluorescence (*36*). Initial experiments using 0.02 mg mL^{-1} bovine complex I, 30 μM NADH, and DHE concentrations up to 100 μM, provided linear reaction rates that did not strongly depend upon the DHE concentration. NADH did not affect detection until concentrations as high as 300 μM were tested. Therefore, the standard assay conditions were 30 μM NADH and 50 μM DHE. Detection was SOD-sensitive; the NADH oxidation activities of both the bovine and *E. coli* enzymes were unaffected by the DHE detection system (their rates of NADH:hexaammine ruthenium oxidoreduction were unchanged); and complex I did not interfere with the detection of superoxide produced by the xanthine/xanthine oxidase system. Unfortunately, superoxide and H_2O_2 could not be detected in the same experiment, because DHE interferes with the Amplex Red detection system (even in control experiments using known aliquots of H_2O_2).

The rate of ethidium production linearly depended upon the concentrations of both bovine and *E. coli* complex I at low concentrations and then started to plateau at higher concentrations. In Figure 5, ethidium production is plotted against H_2O_2 production, measured using Amplex Red. To determine the rate of superoxide production by *E. coli* complex I, we used the bovine enzyme as a standard and determined the factor by which the *E. coli* abscissa needed to be divided, to map the *E. coli* data set onto the bovine data set. The highest correlation was observed using factors from 6−9. A factor of 8 was obtained from comparing the gradients from linear regression at low complex I concentrations. Of the total H_2O_2 produced by bovine complex I, approximately 90% is from superoxide dismutation and only 10% is produced directly. At an equivalent rate of total H_2O_2 production, *E. coli* complex I produces 6−9 times less

Table 3: Comparison of the Rates of Superoxide Formation, H_2O_2 Formation, and O_2 Reduction by Bovine and *E. coli* Complex I

complex I	rate of direct H_2O_2 formation (min^{-1})	rate of superoxide formation (min^{-1})	rate of O_2 reduction (min^{-1})	fraction of total H_2O_2 formed by superoxide dismutation	fraction of O_2 reduced only to superoxide
E. coli	20.4–21.6	4.8–7.2	26.4−27.6	0.1–0.15	0.18–0.26
bovine (*14*)	2.1	37.8	39.9	0.9	0.95

[a] Calculations used 24 H_2O_2 min^{-1} for *E. coli* complex I and 21 H_2O_2 min^{-1} for bovine complex I (Table 2).

superoxide. Therefore, only 10−15% of the H_2O_2 produced by *E. coli* complex I is from superoxide dismutation (see Table 3).

Finally, dihydrorhodamine 123 (DHR) reacts with peroxynitrite but not with NO (*46*). Thus, we aimed to use NO, generated in situ by DETA−NONOate, to trap the superoxide (*37*), and DHR, to detect the peroxynitrite (*38*). Two problems were encountered: the signal decreased significantly as the NADH concentration was increased, and the results were not consistent from day to day. By assaying both enzymes on the same day, we obtained a ratio of 7−8 between the relative rate amounts of superoxide produced. Although these results appear to support those from DHE, we do not have confidence in them as a stand alone data set.

In summary, the quantification of superoxide production from *E. coli* complex I was very prone to artifacts. Only one of six methods proved satisfactory, and even this method did not behave ideally; it did not linearly depend upon the enzyme concentration over a large range and could not be used in combination with Amplex Red. Interestingly, ac cyt *c* and coelenterazine worked well with bovine complex I but not with *E. coli* complex I, perhaps because the supernumerary subunits shield the core of the mitochondrial enzyme or alter the charge distribution on its surface.

Different Outcomes of O_2 Reduction in the Bovine and E. coli Complexes I. Although the rate-determining reaction, the bimolecular reaction between the reduced flavin and molecular O_2, is conserved in both the *E. coli* and bovine complexes I, the fate of the nascent superoxide varies significantly (see Table 3). In bovine complex I, it has more than a 95% chance of escaping the active site without being reduced to H_2O_2, but in *E. coli* complex I, it has only a ∼25% chance. There are several possible explanations. Small differences in the environment of the flavin in the *E. coli* enzyme, relative to the bovine enzyme, may stabilize the nascent superoxide in the active site, slowing its escape; protons may be less available in the active site of the bovine enzyme; or subtle electronic effects may slow the spin transition, required because of the triplet state of O_2 (*26–28*). At present, there is insufficient information about the active-site structure to evaluate these possibilities. Alternatively, in the bovine enzyme especially, the electron on the flavin semiquinone may be transferred rapidly away from the active site, making it unavailable for further reduction of the superoxide. Similar mechanisms have been proposed previously, for xanthine oxidase, fumarate reductase, and succinate dehydrogenase (*47, 48*). This possibility is discussed below, with particular attention to the possible role of the [2Fe−2S] cluster N1a (*3*).

It is perhaps most likely that the different outcomes of O_2 reduction in the two enzymes are the result of accident and not design. Otherwise, one must ask why bovine complex I has evolved to produce superoxide and not H_2O_2 directly. Reduction only to superoxide avoids the loss of a second electron from the respiratory chain, and, given the efficiency of SOD in converting superoxide to H_2O_2 anyway, perhaps this is reason enough. Alternatively, a mechanism that rapidly oxidizes the flavin semiquinone during O_2 reduction may operate also during the stepwise reduction of ubiquinone, so that the lifetime of the flavin semiquinone is minimized during normal turnover. One may tentatively suggest that this is important for energy transduction or propose that minimizing the lifetime of the flavin semiquinone helps to prevent O_2 reduction (*3*), but there is little evidence to support these theories at present.

Does [2Fe−2S] Cluster N1a Minimize the Lifetime of the Flavin Semiquinone? [2Fe−2S] cluster N1a has a higher potential in *E. coli* complex I than in bovine complex I (see Table 1), so that it is reduced rather than oxidized in NADH. Consequently, when O_2 is reduced by *E. coli* complex I, cluster N1a cannot accept the electron from the flavin semiquinone and the chance of the electron being transferred to the nascent superoxide is higher: the different properties of [2Fe−2S] cluster N1a correlate with the different outcomes of O_2 reduction. However, suggesting that the electron from the semiquinone is transferred transiently to cluster N1a in bovine complex I raises the question of how it is recovered to free the cluster for the next turnover. In Figure 6, we consider the kinetic and thermodynamic boundaries on a cluster N1a-based mechanism, which minimizes the formation of H_2O_2.

Figure 6 depicts the simplest possible system, comprising only a flavin and a single cluster, representing the flavin and [2Fe−2S] cluster N1a in bovine complex I. The NADH-reduced enzyme, species 2 (denoted {2}), reacts with O_2 to form O_2^- and a flavin semiquinone, {3}. The electron is rapidly sequestered, and O_2^- dissociates ({4} and {5}). At least 95% of the O_2 is reduced only to O_2^-; therefore, the reduction potential of the cluster (coupled to O_2^- dissociation) is probably at least 80 mV above that of the flavin (E_{F1}). Beyond these initial steps, the mechanism becomes more complex. The system may return to {2} by reacting with O_2 (via {6} to {8}) or be reduced by NADH to {9}. After the reduction of O_2 by {9}, a second decision point occurs at {10}. The nascent O_2^- may simply dissociate and return the system to {2} via {11}, but this route suggests that a control mechanism is not required at all or that it may be reduced to H_2O_2 ({12}). Otherwise, the formation of {13} would result in either O_2^- or H_2O_2 production through {14}. Clearly, an additional feature is required at {10} to prevent H_2O_2 formation. One possibility is that electron transfer from the cluster to the flavin semiquinone actually expels the superoxide anion, because the negatively charged, fully reduced flavin cannot coexist with it in the active site (bypassing {13} and returning to {2}). In this case, the reduction potential

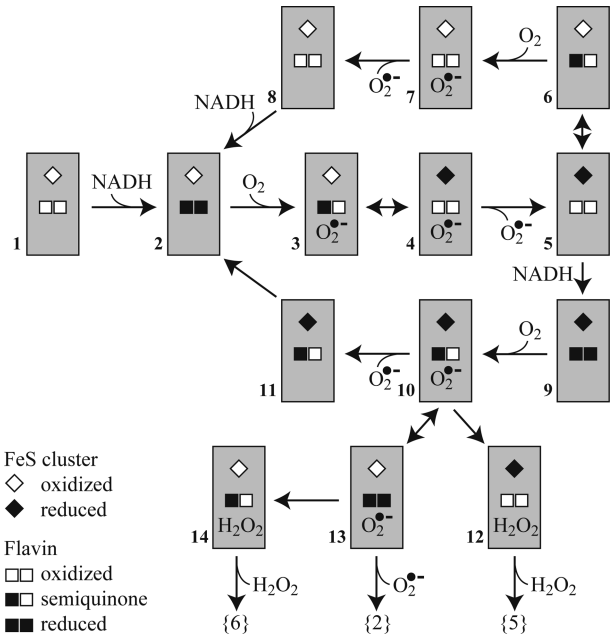

FIGURE 6: Reaction scheme showing how an FeS cluster may minimize the lifetime of a flavin semiquinone. The flavin is reduced by two electrons by NADH and oxidized in one-electron steps by O_2. O_2 is reduced in two one-electron steps to superoxide and then to H_2O_2. Electron transfers between the cluster and the flavin determine the outcome of O_2 reduction (see the text).

of the cluster must be lower than that of the flavin semiquinone (E_{F2}), coupled to O_2^- dissociation. The "binding energy" of O_2^- is unknown, but the emerging picture is that the two flavin potentials must be crossed significantly ($E_{F1} < E_{F2}$) with the cluster potential between them.

In bovine complex I, the potentials of the flavin are crossed by ~90 mV but the potential of [2Fe−2S] cluster N1a is considerably more negative than their average potential (see Table 1). Interestingly, Figure 6 suggests that, if cluster N1a does sequester the electron of semiquinone, it should be ~50% reduced during turnover with O_2 and NADH, but EPR signal N1a has not been observed in NADH-reduced bovine complex I. The idea that cluster N1a, having no apparent role in energy transduction, has an alternative role in minimizing the lifetime of the flavin semiquinone is obviously attractive, and the fate of the nascent superoxide does correlate with its potential. However, evidence to support a causative relationship is lacking thus far. The [2Fe−2S] cluster in the 75 kDa subunit, for example, has a potential suited to the mechanism in Figure 6, or the clusters may act as an ensemble. It is known that the electrons distribute differently between the clusters in the NADH-reduced bovine and *E. coli* complexes I (*49*), so that the individual cluster potentials, intercluster interactions, and two flavin potentials probably all contribute to the relative thermodynamic stability of the flavin semiquinone in the *E. coli* enzyme. Note that the fully reduced flavin in fumarate reductase produces either H_2O_2 or superoxide also, depending upon the oxidation state of the proximal [2Fe−2S] cluster (*48*); this cluster is involved directly in catalysis, lending no support to the idea that a specific cluster is required. In summary, our evidence is broadly consistent with a mechanism in which [2Fe−2S] cluster N1a minimizes the lifetime of the semiquinone radical, but it does not prove the operation of such a mechanism. It is also possible that cluster N1a plays no specific role in the function of complex I but that it contributes to the stability or structure of the enzyme or was simply included as a "bystander" during the modular construction of the contemporary enzyme.

ACKNOWLEDGMENT

We thank Drs. Lothar Kussmaul and Richard J. Shannon for advice and helpful discussions.

REFERENCES

1. Hirst, J. (2005) Energy transduction by respiratory complex I—An evaluation of current knowledge. *Biochem. Soc. Trans. 33*, 525–529.
2. Brandt, U. (2006) Energy converting NADH:quinone oxidoreductase (complex I). *Annu. Rev. Biochem. 75*, 69–92.
3. Sazanov, L. A. (2007) Respiratory complex I: Mechanistic and structural insights provided by the crystal structure of the hydrophilic domain. *Biochemistry 46*, 2275–2288.
4. Raha, S., and Robinson, B. H. (2000) Mitochondria, oxygen free radicals, disease and ageing. *Trends Biochem. Sci. 25*, 502–508.
5. Votyakova, T. V., and Reynolds, I. J. (2001) $\Delta\psi_m$-dependent and -independent production of reactive oxygen species by rat brain mitochondria. *J. Neurochem. 79*, 266–277.
6. Brand, M. D., Affourtit, C., Esteves, T. C., Green, K., Lambert, A. J., Miwa, S., Pakay, J. L., and Parker, N. (2004) Mitochondrial superoxide: Production, biological effects, and activation of uncoupling proteins. *Free Radical Biol. Med. 37*, 755–767.
7. Balaban, R. S., Nemoto, S., and Finkel, T. (2005) Mitochondria, oxidants, and aging. *Cell 120*, 483–495.
8. Wallace, D. C. (2005) A mitochondrial paradigm of metabolic and degenerative diseases, aging and cancer: A dawn for evolutionary medicine. *Annu. Rev. Genet. 39*, 359–407.
9. Lin, M. T., and Beal, M. F. (2006) Mitochondrial dysfunction and oxidative stress in neurodegenerative diseases. *Nature 443*, 787–795.
10. Perier, C., Tieu, K., Guégan, C., Caspersen, C., Jackson-Lewis, V., Carelli, V., Martinuzzi, A., Hirano, M., Przedborski, S., and Vila, M. (2005) Complex I deficiency primes Bax-dependent neuronal apoptosis through mitochondrial oxidative damage. *Proc. Natl. Acad. Sci. U.S.A. 102*, 19126–19131.
11. Adam-Vizi, V., and Chinopoulos, C. (2006) Bioenergetics and the formation of mitochondrial reactive oxygen species. *Trends Pharmacol. Sci. 27*, 639–645.
12. Yadava, N., and Nicholls, D. G. (2007) Spare respiratory capacity rather than oxidative stress regulates glutamate excitotoxicity after partial respiratory inhibition of mitochondrial complex I with rotenone. *J. Neurosci. 27*, 7310–7317.
13. Koopman, W. J. H., Verkaart, S., Visch, H. J., van Emst-de Vries, S., Nijtmans, L. G. J., Smeitink, J. A. M., and Willems, P. H. G. M. (2007) Human NADH:ubiquinone oxidoreductase deficiency: Radical changes in mitochondrial morphology? *Am. J. Physiol. Cell Physiol. 293*, C22–C29.
14. Kussmaul, L., and Hirst, J. (2006) The mechanism of superoxide production by NADH:ubiquinone oxidoreductase (complex I) from bovine heart mitochondria. *Proc. Natl. Acad. Sci. U.S.A. 103*, 7607–7612.
15. Galkin, A., and Brandt, U. (2005) Superoxide radical formation by pure complex I (NADH:ubiquinone oxidoreductase) from *Yarrowia lipolytica*. *J. Biol. Chem. 280*, 30129–30135.
16. Kushnareva, Y., Murphy, A. N., and Andreyev, A. (2002) Complex I-mediated reactive oxygen species generation: Modulation by cytochrome *c* and $NAD(P)^+$ oxidation−reduction state. *Biochem. J. 368*, 545–553.
17. Liu, Y., Fiskum, G., and Schubert, D. (2002) Generation of reactive oxygen species by the mitochondrial electron transport chain. *J. Neurochem. 80*, 780–787.
18. Starkov, A. A., and Fiskum, G. (2003) Regulation of brain mitochondrial H_2O_2 production by membrane potential and NAD(P)H redox state. *J. Neurochem. 86*, 1101–1107.
19. Kudin, A. P., Bimpong-Buta, N. Y.-B., Vielhaber, S., Elger, C. E., and Kunz, W. S. (2004) Characterisation of superoxide-producing sites in isolated brain mitochondria. *J. Biol. Chem. 279*, 4127–4135.
20. Lambert, A. J., and Brand, M. D. (2004) Inhibitors of the quinone-binding site allow rapid superoxide production from mitochondrial

NADH:ubiquinone oxidoreductase (complex I). *J. Biol. Chem. 279*, 39414–39420.
21. Yano, T., Dunham, W. R., and Ohnishi, T. (2005) Characterization of the $\Delta\mu_{H^+}$-sensitive ubisemiquinione species (SQ_{Nf}) and the interaction with cluster N2: New insight into the energy-coupled electron transfer in complex I. *Biochemistry 44*, 1744–1754.
22. Leif, H., Sled, V. D., Ohnishi, T., Weiss, H., and Friedrich, T. (1995) Isolation and characterization of the proton-translocating NADH:ubiquinone oxidoreductase from *Escherichia coli*. *Eur. J. Biochem. 230*, 538–548.
23. Ohnishi, T. (1998) Iron−sulfur clusters/semiquinones in complex I. *Biochim. Biophys. Acta 1364*, 186–206.
24. Zu, Y., Di Bernardo, S., Yagi, T., and Hirst, J. (2002) Redox properties of the [2Fe−2S] center in the 24 kDa (NQO2) subunit of NADH:ubiquinone oxidoreductase (complex I). *Biochemistry 41*, 10056–10069.
25. Sled, V. D., Rudnitzky, N. I., Hatefi, Y., and Ohnishi, T. (1994) Thermodynamic analysis of flavin in mitochondrial NADH: ubiquinone oxidoreductase (complex I). *Biochemistry 33*, 10069–10075.
26. Massey, V. (1994) Activation of molecular oxygen by flavins and flavoproteins. *J. Biol. Chem. 269*, 22459–22462.
27. Klinman, J. P. (2001) Life as aerobes: Are there simple rules for activation of dioxygen by enzymes? *J. Biol. Inorg. Chem. 6*, 1–13.
28. Mattevi, A. (2006) To be or not to be an oxidase: Challenging the oxygen reactivity of flavoenzymes. *Trends Biochem. Sci. 31*, 276–283.
29. Sazanov, L. A., and Hinchliffe, P. (2006) Structure of the hydrophilic domain of respiratory complex I from *Thermus thermophilus*. *Science 311*, 1430–1436.
30. Sazanov, L. A., Carroll, J., Holt, P., Toime, L., and Fearnley, I. M. (2003) A role for native lipids in the stabilization and two-dimensional crystallization of the *Escherichia coli* NADH−ubiquinone oxidoreductase (complex I). *J. Biol. Chem. 278*, 19483–19491.
31. Sherwood, S., and Hirst, J. (2006) Investigation of the mechanism of proton translocation by NADH:ubiquinone oxidoreductase (complex I) from bovine heart mitochondria: Does the enzyme operate by a Q-cycle mechanism? *Biochem. J. 400*, 541–550.
32. Burch, H. B. (1957) Fluorimetric assay of FAD, FMN and riboflavin. *Methods Enzymol. 3*, 960–962.
33. Ukeda, H., Shimamura, T., Tsubouchi, M., Harada, Y., Nakai, Y., and Sawamura, M. (2002) Spectrophotometric assay of superoxide anion formed in Maillard reaction based on highly water-soluble tetrazolium salt. *Anal. Sci. 18*, 1151–1154.
34. Faulkner, K., and Fridovich, I. (1993) Luminol and lucigenin as detectors for $O_2^{\bullet-}$. *Free Radical Biol. Med. 15*, 447–451.
35. Lucas, M., and Solano, F. (1992) Coelenterazine is a superoxide anion-sensitive chemiluminescent probe: Its usefulness in the assay of respiratory burst in neutrophils. *Anal. Biochem. 206*, 273–277.
36. Robinson, K. M., Janes, M. S., Pehar, M., Monette, J. S., Ross, M. F., Hagen, T. M., Murphy, M. P., and Beckman, J. S. (2006) Selective fluorescent imaging of superoxide *in vivo* using ethidium-based probes. *Proc. Natl. Acad. Sci. U.S.A. 103*, 15038–15043.
37. Pryor, W. A., and Squadrito, G. L. (1995) The chemistry of peroxynitrite: A product from the reaction of nitric oxide and superoxide. *Am. J. Physiol. 268*, L699–L722.
38. Kooy, N. W., Royall, J. A., Ischiropoulos, H., and Beckman, J. S. (1994) Peroxynitrite-mediated oxidation of dihydrorhodamine 123. *Free Radical Biol. Med. 16*, 149–156.
39. Hirst, J., Carroll, J., Fearnley, I. M., Shannon, R. J., and Walker, J. E. (2003) The nuclear encoded subunits of complex I from bovine heart mitochondria. *Biochim. Biophys. Acta 1604*, 135–150.
40. Halliwell, B., and Gutteridge, J. M. C. (1998) *Free Radicals in Biology and Medicine*, 3rd ed., Oxford University Press, New York.
41. Imlay, J. A., and Fridovich, I. (1991) Assay of metabolic superoxide production in *Escherichia coli*. *J. Biol. Chem. 266*, 6957–6965.
42. Messner, K. R., and Imlay, J. A. (1999) The identification of primary sites of superoxide and hydrogen peroxide formation in the aerobic respiratory chain and sulfite reductase complex of *Escherichia coli*. *J. Biol. Chem. 274*, 10119–10128.
43. Sinegina, L., Wikström, M., Verkhovsky, M. I., and Verkhovskaya, M. L. (2005) Activation of isolated NADH:ubiquinone reductase I (complex I) from *Escherichia coli* by detergent and phospholipids. Recovery of ubiquinone reductase activity and changes in EPR signals of iron−sulfur clusters. *Biochemistry 44*, 8500–8506.
44. Tarpey, M. M., and Fridovich, I. (2001) Methods of detection of vascular reactive species: Nitric oxide, superoxide, hydrogen peroxide, and peroxynitrite. *Circ. Res. 89*, 224–236.
45. Münzel, T., Afanas'ev, I. B., Kleschyov, A. L., and Harrison, D. G. (2002) Detection of superoxide in vascular tissue. *Arterioscler., Thromb., Vasc. Biol.* 1761–1768.
46. Halliwell, B., and Whiteman, M. (2004) Measuring reactive species and oxidative damage *in vivo* and in cell culture: How should you do it and what do the results mean? *Br. J. Pharmacol. 142*, 231–255.
47. Hille, R., and Massey, V. (1981) Studies on the oxidative half-reaction of xanthine oxidase. *J. Biol. Chem. 256*, 9090–9095.
48. Messner, K. R., and Imlay, J. A. (2002) Mechanism of superoxide and hydrogen peroxide formation by fumarate reductase, succinate dehydrogenase and aspartate oxidase. *J. Biol. Chem. 277*, 42563–42571.
49. Yakovlev, G., Reda, T., and Hirst, J. (2007) Reevaluating the relationship between EPR spectra and enzyme structure for the iron−sulfur clusters in NADH:quinone oxidoreductase. *Proc. Natl. Acad. Sci. U.S.A. 104*, 12720–12725.

BI702243B